

Antiferroelectric Behavior in Symmetric $\text{KNbO}_3/\text{KTaO}_3$ Superlattices

J. Sigman and D. P. Norton

*Department of Materials Science and Engineering, University of Florida, P.O. Box 116400,
Rhines Hall, Gainesville, Florida 32611*

H. M. Christen, P. H. Fleming, and L. A. Boatner

Solid State Division, Oak Ridge National Laboratory, P.O. Box 2008, Oak Ridge, Tennessee 37831

(Received 12 December 2001; published 15 February 2002)

Antiferroelectric behavior is observed in artificially layered $\text{KTaO}_3/\text{KNbO}_3$ perovskite superlattices. While KTaO_3 and KNbO_3 are ferroelectric and paraelectric, respectively, the superlattice appears antiferroelectric based on an increase in the dielectric constant with applied dc bias. This dielectric behavior is inconsistent with the nonlinear response for either paraelectric or ferroelectric materials. However, an increase in the dielectric constant with applied electric field is consistent with antiferroelectric behavior. The antiferroelectric ordering appears to be induced by cation modulation imposed by the superlattice.

DOI: 10.1103/PhysRevLett.88.097601

PACS numbers: 77.84.-s, 77.80.-e

In insulating materials, the dielectric properties are determined by the polarization behavior. The random alignment of dipoles yields a paraelectric response; parallel or antiparallel ordering results in ferroelectric or antiferroelectric behavior, respectively. Controlling the nature of dipole polarization is the key to tailoring material performance. In bulk materials, the manipulation of dielectric properties is typically achieved via doping or control of microstructure. However, since the range of interactions responsible for polarization behavior is larger than the nearest-neighbor atomic spacing, the formation of artificially layered structures offers opportunities to probe, manipulate, and even nanoengineer dielectric material properties.

In this paper, we report on the manipulation of polarization ordering in the $\text{K}(\text{Nb}_x\text{Ta}_{1-x})\text{O}_3$ (KTN) perovskite system via superlattice formation. Among the dielectric materials, the mixed-oxide compound $\text{K}(\text{Nb}_x\text{Ta}_{1-x})\text{O}_3$ is a near-ideal material for both understanding and manipulating the dielectric properties of perovskites [1–3]. KTN is similar to $(\text{Sr},\text{Ba})\text{TiO}_3$ in that, as the composition is altered, the solid solution exhibits a continuous transition from a paraelectric to a ferroelectric material. Pure KTaO_3 is cubic ($a_{300\text{K}} = 3.9885 \text{ \AA}$) and paraelectric at all temperatures. Decreasing the temperature results in a softening of the TO_1 transverse optic, zone-center phonon branch. The soft mode is stabilized by zero-point quantum fluctuations, however, so that KTaO_3 does not undergo a ferroelectric transition but remains cubic and paraelectric down to 0 K. Hence KTaO_3 exhibits so-called “incipient ferroelectric” or “quantum ferroelectric” behavior [4,5]. Pure KNbO_3 , in contrast, exhibits a first-order ferroelectric phase transition accompanied by a change from the cubic to the tetragonal structure at 701 K ($a_p = 4.02 \text{ \AA}$ along $[100]_p$ and $[010]_p$ directions, and $c_p = 3.97 \text{ \AA}$ along the $[001]_p$). Upon further cooling, the structure changes to orthorhombic at 498 K, with lattice param-

eters $a = 5.696 \text{ \AA}$, $b = 5.7213 \text{ \AA}$, and $c = 3.9739 \text{ \AA}$. For the ferroelectric state, the polarization direction is along the $[010]$ (b axis). As a solid solution, the KTN Curie temperature varies continuously according to the formula $T_c = 676x + 32$ (for $x > 4.7\%$). For $x > 0.35$, the solid solution exhibits a first-order ferroelectric phase transition similar to KNbO_3 . Because of its low dielectric loss, high saturation polarization, large electro-optic effects, and low driving voltage for modulation, $\text{KTa}_{1-x}\text{Nb}_x\text{O}_3$ is an attractive material for applications involving holographic data storage, parametric oscillators, pyroelectric detectors, and second harmonic generators [6–9].

Recent developments in oxide film growth provide the opportunity to understand, control, and manipulate the growth of epitaxial oxide films and multilayers in the KTN system at the atomic scale [10,11]. Specifically, the properties of symmetric $\text{KNbO}_3/\text{KTaO}_3$ superlattices grown by pulsed laser deposition on KTaO_3 (001) have been studied [12–14]. Excellent film flatness and crystallinity are evidenced in these films, and the interfaces are found to be compositionally sharp on an atomic scale. Unlike $(\text{Sr},\text{Ba})\text{TiO}_3$, the $\text{K}(\text{Nb},\text{Ta})\text{O}_3$ system displays very little change in the average d spacing in moving across the alloy composition. This significantly minimizes the effects of strain in superlattices, and permits the synthesis of commensurate structures with low defect density. Previous work has shown that, while relatively thick KNbO_3 films are characterized by an orthorhombic structure, $\text{KTaO}_3/\text{KNbO}_3$ superlattices can be uniformly strained in-plane without misfit dislocations, imposing an in-plane KNbO_3 lattice spacing that is identical to that of the KTaO_3 substrate. Temperature-dependent x-ray diffraction measurements indicate a tetragonal-to-tetragonal phase transition for superlattices [15–17] with the structural phase transition temperature, T_c , dependent on the KNbO_3 layer thickness. As the

superlattice period decreases, a reduction of T_c is observed. For symmetric superlattices with periodicities of 50 Å or less, the structural phase transition temperature is identical to that of the $\text{K}(\text{Ta}_{0.5}\text{Nb}_{0.5})\text{O}_3$ random alloy film.

In order to elucidate the properties of these structures, we have investigated the temperature-dependent dielectric response of $\text{KTaO}_3/\text{KNbO}_3$ superlattices, focusing on $1\text{-unit-cell} \times 1\text{-unit-cell}$ (1×1) superlattice structures. The dielectric properties were measured using interdigitated capacitors, with specific attention given to the dielectric behavior near the structural phase transition as observed in the x-ray diffraction results reported earlier [12–14]. The dielectric response of (1×1) $\text{KTaO}_3/\text{KNbO}_3$ superlattices and $\text{K}(\text{Ta}_{0.5}\text{Nb}_{0.5})\text{O}_3$ alloy films was studied at frequencies of 100 kHz and 1 MHz by measuring the capacitance of interdigitated Au/Cr electrodes deposited on the film surface. The epitaxial structures were deposited by pulsed-laser deposition as previously described [13]. The electrode finger separation and width for the interdigitated electrodes were 10 μm . Each capacitor structure consisted of 26 fingers. The capacitance was measured as a function of temperature from 25 to 300 °C in air. This temperature range encompasses the structural transition temperature (~ 200 °C) for the (1×1) $\text{KTaO}_3/\text{KNbO}_3$ superlattices and $\text{K}(\text{Ta}_{0.5}\text{Nb}_{0.5})\text{O}_3$ alloy films as observed in previous x-ray diffraction data. In addition to zero-bias measurements, the dc voltage tunability was measured over this temperature range by measuring the capacitance with applied dc bias voltages ranging from 5 to -5 V.

The temperature-dependent capacitance for a (1×1) $\text{KTaO}_3/\text{KNbO}_3$ superlattice structure, measured at 100 kHz, is shown in Fig. 1(a). A weak, but discernable, local maximum in capacitance is observed at ~ 200 °C, which corresponds with the structural transition. However, the capacitance behavior with applied bias reveals a more complex behavior. Figure 1(a) shows the temperature-dependent capacitance taken with applied dc bias voltages of 0 and 4.7 V. For temperatures less than approximately 140 °C, the capacitance is nearly temperature independent with no discernable bias voltage dependence for dc voltages less than 5 V. This is consistent with a film that is either ferroelectric or paraelectric, given that the electric field strength is only 2 kV/cm. From the phase diagram for $\text{K}(\text{Ta},\text{Nb})\text{O}_3$ and the x-ray diffraction results reported earlier, we anticipate that the film is ferroelectric in this temperature regime. However, as the sample temperature is increased above 140 °C, the capacitance shows an anomalous increase with applied dc voltage as seen in Figs. 1(a) and 1(b). This “positive tunability” in the superlattices with applied bias is clearly seen in the capacitance versus dc bias voltage plots at fixed temperatures, shown in Fig. 1(b). This behavior is unexpected since the application of a dc electric field results in a decrease

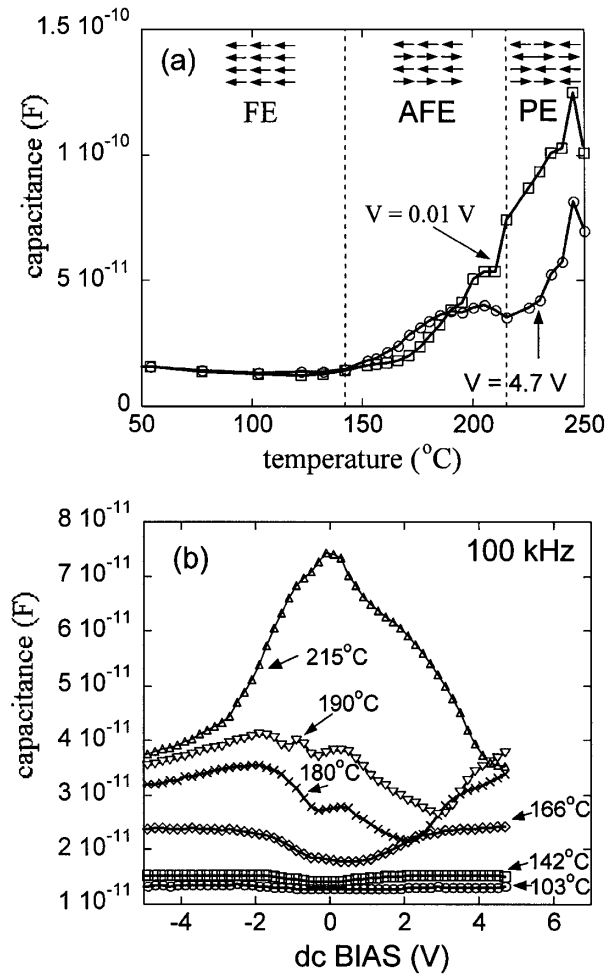


FIG. 1. Capacitance measurements for a 1×1 $\text{KTaO}_3/\text{KNbO}_3$ superlattice structure showing (a) capacitance versus temperature for 0 and 4.7 V dc bias voltages, as well as (b) capacitance versus dc bias voltage measured at various temperatures. Regions corresponding to ferroelectric (FE), antiferroelectric (AFE), and paraelectric (PE) behavior are labeled.

in the dielectric constant for ferroelectric or paraelectric materials.

For measurements performed at 100 kHz, a maximum in the positive dc bias tunability is observed at approximately 175 °C. As the temperature is increased to ~ 215 °C, a crossover is observed where the tunability becomes negative, indicative of conventional ferroelectric and paraelectric behavior. Note that this crossover temperature for tunability is in the temperature range where the structural phase transition is observed from the temperature-dependent x-ray diffraction data [13,14]. At approximately 230 °C, a “conventional” paraelectric tunability greater than 50% with an applied voltage of 4.7 V is observed. From the results presented in Figs. 1(a) and 1(b), a transition from positive to negative tunability is observed as the temperature is increased.

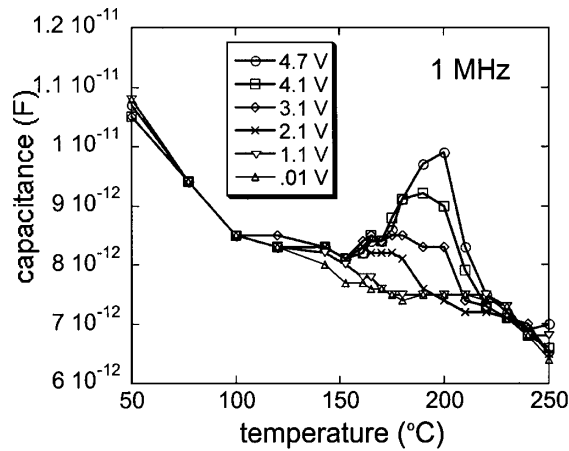


FIG. 2. Capacitance versus temperature for a 1×1 $\text{KTaO}_3/\text{KNbO}_3$ superlattice structure with various dc bias voltages applied. Measurements were performed at 1 MHz.

The temperature-dependent capacitance was also measured at 1 MHz for the same 1×1 $\text{KTaO}_3/\text{KNbO}_3$ superlattice sample and the results are shown in Fig. 2. Again, a large positive tunability is observed. For $\nu = 1$ MHz, the positive tunability is pronounced only at the temperature corresponding to the structural phase transition. While the zero-bias capacitance curve shows no identifiable structure suggesting a phase transition, the biased curves clearly show evidence for a transition at $\sim 195^\circ\text{C}$.

Similar measurements of the temperature-dependent capacitance with applied dc bias voltage were performed on $\text{K}(\text{Ta}_{0.5}\text{Nb}_{0.5})\text{O}_3$ alloy films. The alloy film does not exhibit this anomalous tunability behavior. Changes in the slope of the temperature-dependent capacitance are observed at 190°C , corresponding to the structural phase transition. Since the average film composition is the same in both the alloy and the superlattice film, the discrepancy in the tunability behavior must be associated with the artificial ordering.

An increase in the dielectric constant (observed via capacitance measurements) with applied dc electric field is inconsistent with the expected behavior for either a paraelectric or ferroelectric material [15]. However, the observed behavior for the 1×1 $\text{KTaO}_3/\text{KNbO}_3$ superlattices is remarkably similar to that for antiferroelectric perovskites [16–19]. An increase in the dielectric constant with applied field is a signature behavior indicating antiferroelectric ordering. An antiferroelectric is characterized by an antiparallel ordered array of local dipoles. It can be viewed as two interpenetrating sublattices of equal and opposite polarization with no net spontaneous polarization. In many cases, the antiferroelectric ordering of dipoles can be transformed to ferroelectric ordering via the application of an electric field. This is the origin of the increase in the dielectric constant with applied dc voltage. The difference in free energy between ferroelectric and antiferroelectric phases can be quite small. An additional signature of antiferroelectric behavior is a hysteresis in

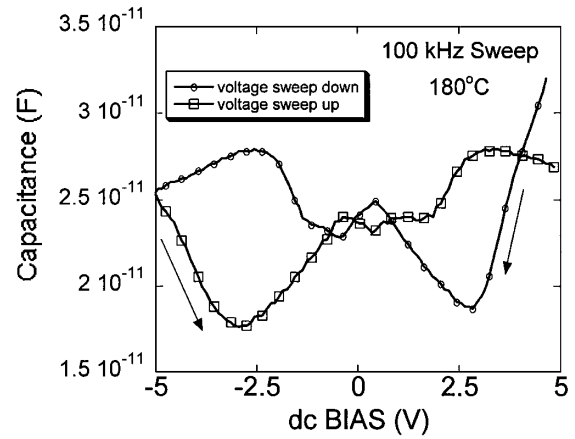


FIG. 3. Trace of the capacitance as the voltage is swept from +5 V to -5 V, then back to +5 V showing hysteretic behavior.

the dielectric constant versus field behavior as voltage is swept between positive and negative polarity. Figure 3 shows a trace of the capacitance vs voltage for a 1×1 $\text{KTaO}_3/\text{KNbO}_3$ superlattice at 180°C . A clear hysteresis is observed.

Based on the tunability behavior, a reasonable description of the superlattice dielectric properties is as follows. Below approximately 140°C , relative insensitivity of the dielectric in the 1×1 superlattice is consistent with a ferroelectric phase. This assumption is based on the typical phase development of antiferroelectrics, where ferroelectricity is observed at temperatures below the antiferroelectric regime. This is also consistent with the bulk behavior of $\text{K}(\text{Ta},\text{Nb})\text{O}_3$ alloys. As the temperature is raised above $\sim 140^\circ\text{C}$, an antiferroelectric phase is observed. For temperatures greater than 230°C , the superlattice becomes paraelectric.

It is interesting to consider the origin of antiferroelectric behavior in superlattice structures whose constituent compounds are ferroelectric or paraelectric. For several complex perovskite materials (e.g., $\text{Pb}_2\text{B}'\text{B}''\text{O}_6$) in which multiple *B*-site cations order into a superstructure, antiferroelectric behavior is observed [20,21]. In fact, for many of these compounds, the antiferroelectric phase correlates directly with the *B*-site superstructure. Cation substitution that randomizes *B*-site ordering also suppresses antiferroelectric behavior. This is true even for solid solutions in which the two end members are antiferroelectric, as seen in $\text{Pb}(\text{Yb}_{1/2}\text{Ta}_{1/2})\text{O}_3$ - $\text{Pb}(\text{Lu}_{1/2}\text{Nb}_{1/2})\text{O}_3$ [22]. With the $\text{KTaO}_3/\text{KNbO}_3$ superlattices, *B*-site cation modulation is artificially imposed. The resulting change in free energy apparently favors antiferroelectric dipole alignment. Understanding the nature of the interaction that leads to antiparallel dipole orientation will require theoretical calculations of the dipole configuration free energy. The characterization of additional symmetric and asymmetric superlattice structures will also be useful in understanding these results.

This work was supported by the Army Research Office through research Grant No. DAAD 19-01-1-0508. Oak Ridge National Laboratory is managed by UT-Battelle, LLC, for the U.S. DOE under Contract No. DE-AC05-00OR22725.

-
- [1] D.G. Bozinis and J.P. Hurrell, Phys. Rev. B **13**, 3109 (1976).
- [2] Y. Fujii and T. Sakudo, J. Phys. Soc. Jpn. **41**, 888 (1976).
- [3] J. Toulouse, X.M. Wang, L. A. Knass, and L. A. Boatner, Phys. Rev. B **43**, 8297 (1991).
- [4] U. T. Höchli, H. E. Weibel, and L. A. Boatner, Phys. Rev. Lett. **39**, 1158 (1977).
- [5] U. T. Höchli and L. A. Boatner, Phys. Rev. B **20**, 266 (1979).
- [6] F. S. Galasso, *Perovskites and High T_c Superconductors* (Gordon and Breach, New York, 1990).
- [7] D. Rytz, M. B. Klein, B. Bobbs, M. Matloubian, and H. Fetterman, Jpn. J. Appl. Phys. **24**, Suppl. 24-2, 1010 (1985).
- [8] A. C. Carter, J. S. Horvitz, D. B. Chrisey, J. M. Pond, S. W. Kirchoefer, and W. Chang, Integr. Ferroelectr. **17**, 273 (1997).
- [9] H. Khemakhem, J. Ravez, and A. Daoud, Phys. Status Solidi (a) **161**, 557 (1997).
- [10] S. Yilmaz, T. Venkatesan, and R. Gerhard-Multhaupt, Appl. Phys. Lett. **58**, 2479 (1991).
- [11] F. E. Fernandez, M. Pumarol, P. Marrero, E. Rodriguez, and H. A. Mourad, Mater. Res. Soc. Symp. Proc. **493**, 365 (1998).
- [12] H.-M. Christen, L. A. Boatner, J. D. Budai, M. F. Chisholm, L. A. Gea, P. J. Marrero, and D. P. Norton, Appl. Phys. Lett. **68**, 1488 (1996).
- [13] H.-M. Christen, E. D. Specht, D. P. Norton, M. F. Chisholm, and L. A. Boatner, Appl. Phys. Lett. **72**, 2535 (1998).
- [14] E. D. Specht, H.-M. Christen, D. P. Norton, and L. A. Boatner, Phys. Rev. Lett. **80**, 4317 (1998).
- [15] W. Chang, J. S. Horvitz, W.-J. Kim, J. M. Pond, S. W. Kirchoefer, C. M. Gilmore, S. B. Qadri, and D. B. Chrisey, Mater. Res. Soc. Symp. Proc. **541**, 693 (1999).
- [16] G. A. Smolenskii, V. A. Bokov, V. A. Isupov, N. N. Krainik, R. E. Pasynkov, and A. I. Sokolov, *Ferroelectrics and Related Materials* (Gordon and Breach, London, 1984), pp. 607–659.
- [17] B. Xu, L. E. Cross, and J. J. Bernstein, Thin Solid Films **377–378**, 712 (2000).
- [18] S. Chattopadhyay, P. Ayyub, V. R. Palkar, M. S. Multani, S. P. Pai, S. C. Purandare, and R. Pinto, J. Appl. Phys. **83**, 7808 (1998).
- [19] S. S. N. Bharadwaja and S. B. Krupanidhi, J. Appl. Phys. **86**, 5862 (1999).
- [20] J. R. Kwon and W. K. Choo, J. Phys. Condens. Matter **3**, 2147 (1991).
- [21] A. A. Bokov, I. P. Raevskii, and V. G. Smotrakov, Sov. Phys. Solid State **25**, 1168 (1983).
- [22] Y. Park and K. Cho, J. Am. Ceram. Soc. **83**, 135 (2000).